Tensor Product Model Based Control of a Three Degrees-of-Freedom Aeroelastic Model

Béla Takarics[1] and Péter Baranyi[2]
Computer and Automation Research Institute of the

Hungarian Academy of Sciences, H-1111 Budapest, Hungary

I. Introduction

Active control of aeroelasticity has been in the focus of aerospace and control engineering for several decades. An introduction to this topic can be found in [1]. This paper largely focuses on the three degrees-of-freedom (DoF) Nonlinear Aeroelastic Test Apparatus (NATA) model. The NATA model with unsteady aerodynamics was presented in [2, 3] and several active controllers were developed in [4–14]. LPV control of an improved three DoF aeroelastic model is discussed in [15].

The aim of this paper is to propose a control design strategy to stabilize the improved 3 DoF NATA model presented in [15], as well as to stabilize the NATA model with nonlinear friction. It is assumed that only the free stream velocity and the pitch angle are measurable, thus an output feedback control structure is applied. The control design considers the following performance requirements: asymptotic stability, decay rate and constraint on the control signal, which are formulated in terms of Linear Matrix Inequalities (LMIs). The proposed control design strategy has two main steps. First, the quasi linear parameter varying (qLPV) NATA model is transformed into Tensor Product (TP) type polytopic form via TP model transformation ([16–18]). LMI based control design is applied to the TP type polytopic form in the second step, which yields in stabilising controller and observer via optimising the control performance.

Besides resulting in a stabilising control solution to the 3 DoF NATA model, it is shown that

---

[1] Research fellow, 3D Internet-based Control and Communications Laboratory, Computer and Automation Research Institute, Hungarian Academy of Sciences, Kende utca 13-17, H-1111 Budapest, Hungary.
[2] Head of Laboratory, 3D Internet-based Control and Communications Laboratory, Computer and Automation Research Institute, Hungarian Academy of Sciences.

the proposed control design methodology has the following properties: the control design can be carried out in a non-heuristic, tractable and routine-like fashion; the design steps are the same for the three DoF model as for the two DoF model in [9, 10]; the model can be extended with additional nonlinearities such as friction; a feasible LMI solution is achieved via convex hull manipulation; the control design strategy is also oblivious as to whether the non-linearities are given as analytical formulas, in soft-computing form or as numerical data sets. Numerical simulations are carried out with a perturbed case, where measurement noise, time delay, parameter uncertainties and control signal saturation are present.

The paper is structured as follows: Section II presents the equations of motion and the qLPV model of the three DoF aeroelastic wing section. Section III introduces the proposed control design strategy. Based on the control strategy, Section IV gives the results of the control design, Section V provides simulation results with evaluation and comparison to results of other published solutions. Conclusions are stated at the end of the paper.

II. Equations of Motion of the Three DoF Aeroelastic Wing Section

One of the most recent models of the three DoF aeroelastic wing section based on real measurements, which was adopted in this investigation, was presented and deeply elaborated in [11, 15]. The problem of flutter suppression for the prototypical aeroelastic wing section is considered. The flat plate airfoil is constrained to have three DoF: plunge h, pitch α and trailing-edge surface deflection β. The equations of motion can be written as:

$$\begin{pmatrix} m_h + m_\alpha + m_\beta & m_a x_a b + m_\beta r_\beta + m_\beta x_\beta & m_\beta r_\beta \\ m_a x_a b + m_\beta r_\beta + m_\beta x_\beta & \hat{I}_\alpha + \hat{I}_\beta + m_\beta r_\beta^2 + 2 x_\beta m_\beta r_\beta & \hat{I}_\beta + x_\beta m_\beta r_\beta \\ m_\beta r_\beta & \hat{I}_\beta + x_\beta m_\beta r_\beta \hat{I}_\beta m x_\alpha b & I_\alpha \end{pmatrix} \begin{pmatrix} \ddot{h} \\ \ddot{\alpha} \\ \ddot{\beta} \end{pmatrix} + \tag{1}$$

$$\begin{pmatrix} c_h & 0 & 0 \\ 0 & c_\alpha & 0 \\ 0 & 0 & c_{\beta_{servo}} \end{pmatrix} \begin{pmatrix} \dot{h} \\ \dot{\alpha} \\ \dot{\beta} \end{pmatrix} + \begin{pmatrix} k_h & 0 & 0 \\ 0 & k_\alpha(\alpha) & 0 \\ 0 & 0 & k_{\beta_{servo}} \end{pmatrix} \begin{pmatrix} h \\ \alpha \\ \beta \end{pmatrix} = \begin{pmatrix} -L \\ M \\ k_{\beta_{servo}} \beta_{des} \end{pmatrix}.$$

$k_\alpha(\alpha)$ is obtained in [15] by curve fitting on the measured displacement-moment data for a non-linear spring $k_\alpha(\alpha) = 25.55 - 103.19\alpha + 543.24\alpha^2$. It is important to emphasize that the order of the polynomial defining $k_\alpha(\alpha)$ does not influence the control design methodology, see later. Hence, one can apply a higher order polynomial to model the nonlinearity of the spring, which can be found in previous works dealing with the aeroelastic wing section model ([5]).

Quasi-steady aerodynamic force L and moment M are assumed in the same way as earlier works had done in their control design approaches:

$$L = \rho U^2 b C_{l_\alpha} \left(\alpha + \frac{\dot{h}}{U} + \left(\frac{1}{2} - a \right) b \frac{\dot{\alpha}}{U} \right) + \rho U^2 b c_{l_\beta} \beta \tag{2}$$

$$M = \rho U^2 b^2 C_{m_{\alpha,eff.}} \left(\alpha + \frac{\dot{h}}{U} + \left(\frac{1}{2} - a \right) b \frac{\dot{\alpha}}{U} \right) + \rho U^2 b C_{m_{\beta,eff.}} \beta.$$

The above L and M above are accurate for the low-velocity regime.

Based on [15], it is assumed that the trailing-edge servo-motor dynamics can be represented using a second-order system of the form:

$$\hat{I}_\beta \ddot{\beta} + c_{\beta_{servo}} \dot{\beta} + k_{\beta_{servo}} \beta = k_{\beta_{servo}} \mathbf{u}_\beta. \tag{3}$$

By combining equations (1), (2) and (3) one obtains:

$$\underbrace{\begin{pmatrix} m_h + m_\alpha + m_\beta & m_a x_a b + m_\beta r_\beta + m_\beta x_\beta & m_\beta r_\beta \\ m_a x_a b + m_\beta r_\beta + m_\beta x_\beta & \hat{I}_\alpha + \hat{I}_\beta + m_\beta r_\beta^2 + 2 x_\beta m_\beta r_\beta & \hat{I}_\beta + x_\beta m_\beta r_\beta \\ m_\beta r_\beta & \hat{I}_\beta + x_\beta m_\beta r_\beta \hat{I}_\beta m x_\alpha b & I_\alpha \end{pmatrix}}_{\mathbf{M}_{eom}} \begin{pmatrix} \ddot{h} \\ \ddot{\alpha} \\ \ddot{\beta} \end{pmatrix} + \tag{4}$$

$$+ \underbrace{\begin{pmatrix} c_h + \rho b S C_{l_\alpha} U & \left(\frac{1}{2} - a\right) b \rho b S C_{l_\alpha} U & 0 \\ -\rho b^2 S C_{m_{\alpha,eff}} U & c_\alpha - \left(\frac{1}{2} - a\right) b \rho b^2 S C_{m_{\alpha,eff}} U & 0 \\ 0 & 0 & c_{\beta_{servo}} \end{pmatrix}}_{\mathbf{C}_{eom}} \begin{pmatrix} \dot{h} \\ \dot{\alpha} \\ \dot{\beta} \end{pmatrix} +$$

$$+\underbrace{\begin{pmatrix} k_h & \rho b S C_{l_\alpha} U^2 & \rho b S C_{l_\beta} U^2 \\ 0 & k_\alpha(\alpha) - \rho b^2 S C_{m_{\alpha,eff}} U^2 & -\rho b^2 S C_{m_{\beta,eff}} U^2 \\ 0 & 0 & k_{\beta_{servo}} \end{pmatrix}}_{\mathbf{K}_{eom}} \begin{pmatrix} h \\ \alpha \\ \beta \end{pmatrix} = \underbrace{\begin{pmatrix} 0 \\ 0 \\ k_{\beta_{servo}} \end{pmatrix}}_{\mathbf{F}_{eom}} \mathbf{u}.$$

where $\mathbf{M}_{eom}$, $\mathbf{C}_{eom}$, $\mathbf{K}_{eom}$ and $\mathbf{F}_{eom}$ are the mass, damping, stiffness and forcing matrices of the equation of motion [15].

The above equation can be transformed to state-space qLPV form of:

$$\begin{pmatrix} \dot{\mathbf{x}}(t) \\ \mathbf{y}(t) \end{pmatrix} = \mathbf{S}(\mathbf{p}(t)) \begin{pmatrix} \mathbf{x}(t) \\ \mathbf{u}(t) \end{pmatrix}, \tag{5}$$

with input $\mathbf{u}(t) = u_\beta \in \mathbb{R}$, the measurable output $\mathbf{y}(t) = \alpha \in \mathbb{R}$ and state vector $\mathbf{x}(t) = \begin{pmatrix} \mathbf{x}_1(t) & \mathbf{x}_2(t) & \mathbf{x}_3(t) & \mathbf{x}_4(t) & \mathbf{x}_5(t) & \mathbf{x}_6(t) \end{pmatrix}^T = \begin{pmatrix} \dot{h} & \dot{\alpha} & \dot{\beta} & h & \alpha & \beta \end{pmatrix}^T \in \mathbb{R}^6$. The system matrix

$$\mathbf{S}(\mathbf{p}(t)) = \begin{pmatrix} \mathbf{A}(\mathbf{p}(t)) & \mathbf{B}(\mathbf{p}(t)) \\ \mathbf{C}(\mathbf{p}(t)) & \mathbf{D}(\mathbf{p}(t)) \end{pmatrix} \in \mathbb{R}^{7\times 7} \tag{6}$$

is a parameter-varying object, where $\mathbf{p}(t) = \begin{pmatrix} U(t) & \alpha(t) \end{pmatrix}^T \in \Omega$ and $\Omega = [a_1, b_1] \times [a_2, b_2]$ is a closed hypercube. $\mathbf{p}(t)$ includes α, an element of $\mathbf{x}(t)$, therefore, (6) belongs to the class of qLPV systems.

The elements of $\mathbf{S}(\mathbf{p}(t))$ are:

$$\begin{aligned} \mathbf{A}(\mathbf{p}(t)) &= \begin{pmatrix} -\mathbf{M}_{eom}^{-1}\mathbf{C}_{eom}(\mathbf{p}(t)) & -\mathbf{M}_{eom}^{-1}\mathbf{K}_{eom}(\mathbf{p}(t)) \\ -\mathbf{I} & 0 \end{pmatrix}, \quad \mathbf{B} = \begin{pmatrix} \mathbf{M}_{eom}^{-1}\mathbf{F}_{eom} \\ 0 \end{pmatrix}, \\ \mathbf{C} &= \begin{pmatrix} 0 & 0 & 0 & 0 & 1 & 0 \end{pmatrix} \quad \text{and} \quad \mathbf{D} = 0. \end{aligned} \tag{7}$$

The details and definition of each system parameter can be found in [15] and they have the following values:

$m_h = 6.516kg$; $m_\alpha = 6.7kg$; $m_\beta = 0.537kg$; $x_\alpha = 0.21$; $x_\beta = 0.233$; $r_\beta = 0m$; $a = -0.673m$; $b = 0.1905m$; $\hat{I}_\alpha = 0.126kgm^2$; $\hat{I}_\beta = 10^-5$; $c_h = 27.43Nms/rad$; $c_\alpha = 0.215Nms/rad$; $c_{\beta_{servo}} =$

$4.182 * 10^-4 Nms/rad$; $k_h = 2844$; $k_{\beta_{servo}} = 7.6608 * 10^-3$; $\rho = 1.225 kg/m^3$; $C_{l_\alpha} = 6.757$; $C_{m_{\alpha,eff}} = -1.17$; $C_{l_\beta} = 3.774$; $C_{m_{\beta,eff}} = -2.1$; $S = 0.5945m$.

III. The Proposed Control Design Strategy

A. Reconstruction of the TP type polytopic model

The mathematical background of the TP model transformation and TP model transformation based LMI control design was introduced and elaborated in [16–18] and the methodology was presented in [9, 10] for the two DoF aeroelastic model. The main definitions related to TP model transformation and TP type polytopic models are the following.

Definition 1 *(Finite element TP type polytopic model - TP model):* $\mathbf{S}(\mathbf{p}(t))$ *in (6) is given for any parameter as the parameter-varying convex combination of LTI system matrices* $\mathbf{S} \in \mathbb{R}^{O \times I}$.

$$\mathbf{S}(\mathbf{p}(t)) = \sum_{i_1=1}^{I_1} \sum_{i_2=1}^{I_2} .. \sum_{i_N=1}^{I_N} w_{n,i_n}(p_n(t)) \mathbf{S}_{i_1,i_2,..,i_N} = \mathcal{S} \prod_{n=1}^{N} \mathbf{w}_n \left(p_n\left(t\right)\right), \tag{8}$$

where $\mathbf{p}(t) \in \Omega$. *The (N+2) dimensional coefficient tensor* $\mathcal{S} \in \mathbb{R}^{I_1 \times I_2 \times \cdots \times I_n \times O \times I}$ *is constructed from the LTI vertex systems* $\mathbf{S}_{i_1,i_2,\ldots,i_N}$ *(8) and the row vector* $\mathbf{w}_n\left(p_n\left(t\right)\right)$ *contains one variable and continuous weighting functions* $w_{n,i_n}(p_n(t))$, $i_n = 1 \ldots I_N$. *The weighting functions satisfy the following criteria:*

$$\forall n, i, p_n(t) : w_{n,i}(p_n(t)) \in [0, 1]; \tag{9}$$

$$\forall n, p_n(t) : \sum_{i=1}^{I_n} w_{n,i}(p_n(t)) = 1. \tag{10}$$

Definition 2 *(NO/CNO, NOrmal type TP model): The TP model is NO (normal) type model if its weighting functions are Normal, that is if it satisfies (9), (10), and the largest value of all weighting functions is 1. The convex TP model is CNO (close to normal) if it satisfies (9), (10) and the largest value of all weighting functions is 1 or close to 1.*

Definition 3 *(TP model transformation): TP model transformation is a numerical method to transform qLPV models given in the form of (6) to TP type polytopic model in the form of (8) so that a large class of LMI based control design techniques can be immediately applied. If the original qLPV model has no exact TP representation TP model transformation is capable of finding the TP type*

approximants of arbitrary accuracy. This feature can also be useful for complexity reduction via finding the best lower rank approximation in $\mathcal{L}_2$ sense.

TP model transformation can be executed uniformly (irrespective of whether the model is given in the form of analytical equations resulting from physical considerations or as an outcome of soft computing-based identification techniques such as neural networks or fuzzy logic-based methods, or as a result of a black-box identification etc.), within a reasonable amount of time [17]. Thus, the transformation replaces the analytical, and in many cases complex and not obvious conversions to numerical, tractable and straightforward operations that can be carried out in a routine fashion.

B. Control structure

A large class of LMI based control design techniques is available for polytopic models. The control design technique applied in this research results in a controller and observer, which have the polytopic of the model. It is assumed that not all of the state variables of the NATA model are measurable (in the present research only the pitch angle α is measurable); therefore, output feedback design structure is applied. The observers are required to satisfy $\mathbf{x}(t) - \hat{\mathbf{x}}(t) \to 0 \quad \text{as} \quad t \to \infty$, where $\hat{\mathbf{x}}(t)$ denotes the state-vector estimated by the observer. $\mathbf{p}(t)$ does not contain values from the estimated state-vector $\hat{\mathbf{x}}(t)$, thus, the following strategy for controller and observed design was used ([19, 20]):

$$\begin{aligned}\dot{\hat{\mathbf{x}}}(t) &= \mathbf{A}(\mathbf{p}(t))\hat{\mathbf{x}}(t) + \mathbf{B}(\mathbf{p}(t))\mathbf{u}(t) + \mathbf{K}(\mathbf{p}(t))(\mathbf{y}(t) - \hat{\mathbf{y}}(t)) \\ \hat{\mathbf{y}}(t) &= \mathbf{C}(\mathbf{p}(t))\hat{\mathbf{x}}(t),\end{aligned}$$

where $\mathbf{u}(t) = -\mathbf{F}(\mathbf{p}(t))\mathbf{x}(t)$.

This, takes the following TP type polytopic structure:

$$\begin{aligned}\dot{\hat{\mathbf{x}}}(t) &= \mathcal{A} \underset{n=1}{\overset{N}{\boxtimes}} \mathbf{w}_n(p_n(t))\hat{\mathbf{x}}(t) + \mathcal{B} \underset{n=1}{\overset{N}{\boxtimes}} \mathbf{w}_n(p_n(t))\mathbf{u}(t) + \mathcal{K} \underset{n=1}{\overset{N}{\boxtimes}} \mathbf{w}_n(p_n(t))(\mathbf{y}(t) - \hat{\mathbf{y}}(t)) \\ \hat{\mathbf{y}}(t) &= \mathcal{C} \underset{n=1}{\overset{N}{\boxtimes}} \mathbf{w}_n(p_n(t))\hat{\mathbf{x}}(t) \\ \mathbf{u}(t) &= -\left(\mathcal{F} \underset{n=1}{\overset{N}{\boxtimes}} \mathbf{w}_n(p_n(t))\right)\mathbf{x}(t).\end{aligned} \tag{11}$$

The goal of the design is to determine gains $\mathcal{F}$ and $\mathcal{K}$ in such a way that the stability of the output-feedback control structure is guaranteed. The LTI feedback gains $\mathbf{F}_{i_1,i_2,\ldots,i_N}$ and observer gains $\mathbf{K}_{i_1,i_2,\ldots,i_N}$ stored in tensor $\mathcal{F}$ and $\mathcal{K}$ are called *vertex feedback gains* and *vertex observer gains*, respectively.

C. Control performance optimisation based on LMIs

There are several LMI theorems available for observer and controller design to derive the vertex gains $\mathcal{K}$ of the observer and the feedback gains $\mathcal{F}$ of the controller.

The following control performance requirements were specified:

- Asymptotic stability for the controller and observer;
- Decay rate for the controller;
- Constrain on the control value for the controller.

This paper selects the same LMI theorems as applied for the 2 DoF aeroelastic wing case presented in [9, 10]:

Theorem 1 *(Globally and asymptotically stable observer and controller) Assume the polytopic model (8) with controller and observer structure (11). This output-feedback control structure is globally and asymptotically stable if there exists such* $\mathbf{P}_1 > \mathbf{0}, \mathbf{P}_2 > \mathbf{0}$ *and* $\mathbf{M}_{1,r}, \mathbf{N}_{2,r}$ $(r = 1, \ldots, R$ *and* R *is the number of LTI vertex systems) satisfying equations*

$$\begin{aligned}
\mathbf{P}_1\mathbf{A}_r^T - \mathbf{M}_{1,r}^T\mathbf{B}_r^T + \mathbf{A}_r\mathbf{P}_1 - \mathbf{B}_r\mathbf{M}_{1,r} &< \mathbf{0},\\
\mathbf{A}_r^T\mathbf{P}_2 - \mathbf{C}_r^T\mathbf{N}_{2,r}^T + \mathbf{P}_2\mathbf{A}_r - \mathbf{N}_{2,r}\mathbf{C}_r &< \mathbf{0},\\
\mathbf{P}_1\mathbf{A}_r^T - \mathbf{M}_{1,s}^T\mathbf{B}_r^T + \mathbf{A}_s\mathbf{P}_1 - \mathbf{B}_r\mathbf{M}_{1,s} + \mathbf{P}_1\mathbf{A}_s^T - \mathbf{M}_{1,r}^T\mathbf{B}_s^T + \mathbf{A}_s\mathbf{P}_1 - \mathbf{B}_s\mathbf{M}_{1,r} &< \mathbf{0},\\
\mathbf{A}_r^T\mathbf{P}_2 - \mathbf{C}_s^T\mathbf{N}_{2,r}^T + \mathbf{P}_2\mathbf{A}_r - \mathbf{N}_{2,r}\mathbf{C}_s + \mathbf{A}_s^T\mathbf{P}_2 - \mathbf{C}_r^T\mathbf{N}_{2,s}^T + \mathbf{P}_2\mathbf{A}_s - \mathbf{N}_{2,s}\mathbf{C}_r &< \mathbf{0}
\end{aligned}$$

for $r < s \leq R$*, except the pairs* (r, s) *such that* $\forall \mathbf{p}(t) : w_r(\mathbf{p}(t))w_s(\mathbf{p}(t)) = 0$*, and where* $\mathbf{M}_{1,r} = \mathbf{F}_r\mathbf{P}_1$ *and* $\mathbf{N}_{2,r} = \mathbf{P}_2\mathbf{K}_r$*. The feedback gains and the observer gains can then be obtained from the solution of the above LMIs as* $\mathbf{F}_r = \mathbf{M}_{1,r}\mathbf{P}_1^{-1}$ *and* $\mathbf{K}_r = \mathbf{P}_2^{-1}\mathbf{N}_{2,r}$*.*

Theorem 2 *(Globally and asymptotically stable observer and controller with decay rate)*

$$\begin{aligned}
\mathbf{P}_1\mathbf{A}_r^T - \mathbf{M}_{1,r}^T\mathbf{B}_r^T + \mathbf{A}_r\mathbf{P}_1 - \mathbf{B}_r\mathbf{M}_{1,r} + 2\alpha\mathbf{P}_1 &< \mathbf{0},\\
\mathbf{A}_r^T\mathbf{P}_2 - \mathbf{C}_r^T\mathbf{N}_{2,r}^T + \mathbf{P}_2\mathbf{A}_r - \mathbf{N}_{2,r}\mathbf{C}_r + 2\alpha\mathbf{P}_2 &< \mathbf{0},\\
\mathbf{P}_1\mathbf{A}_r^T - \mathbf{B}_s\mathbf{M}_{1,r} - \mathbf{M}_{1,s}^T\mathbf{B}_r^T + \mathbf{A}_s\mathbf{P}_1 - \mathbf{B}_r\mathbf{M}_{1,s} + \mathbf{P}_1\mathbf{A}_s^T - \mathbf{M}_{1,r}^T\mathbf{B}_s^T + \mathbf{A}_s\mathbf{P}_1 + 4\alpha&\\
\mathbf{P}_1 &< \mathbf{0},\\
\mathbf{A}_r^T\mathbf{P}_2 - \mathbf{C}_s^T\mathbf{N}_{2,r}^T + \mathbf{P}_2\mathbf{A}_r - \mathbf{N}_{2,r}\mathbf{C}_s + \mathbf{A}_s^T\mathbf{P}_2 - \mathbf{C}_r^T\mathbf{N}_{2,s}^T + \mathbf{P}_2\mathbf{A}_s - \mathbf{N}_{2,s}\mathbf{C}_r + 4\alpha\mathbf{P}_2 &< \mathbf{0},
\end{aligned}$$

Solving the LMIs yields asymptotically stable observer and controller with decay rate.

Theorem 3 *(Globally and asymptotically stable observer and controller with constraint on the control value) Simultaneously solving the LMIs of Theorem 1 with Theorem 3 in the form of:*

$$\phi^2\mathbf{I} \leq \mathbf{P}_1$$

$$\begin{pmatrix} \mathbf{P}_1 & \mathbf{M}_r{}^T \\ \mathbf{M}_r & \mu^2\mathbf{I} \end{pmatrix} \geq 0$$

leads to an asymptotically stable controller and observer structure with bounded l_2 norm of the controller.

One can utilise or design further LMIs in order to guarantee various additional constraints.

D. Searching feasibility of LMI tests via convex hull manipulation

LMI based design yields an optimized solution for the given convex hull, rather than for the given qLPV problem, making the control design conservative. As such, the feasibility test of LMIs is sensitive to the actual polytopic form of the model [21], hence both the LMI based optimalisation and the convex hull manipulation must be simultaneously investigated for control system design. A number of different convex models was defined in [10]. SNNN, CNO and IRNO type convex representations were examined in the current investigation, however, only the CNO type representation was able to lead to feasible LMI solution, see later.

IV. Results of the Control Design

A. TP model of the 3 DoF aeroelastic wing section

TP model transformation (generating CNO type weighting functions) is executed on the qLPV state-space model (7). The transformation space Ω is defined in the interval $U \in [8, 20](m/s)$ and $\alpha \in [-0.3, 0.3](rad)$ and the grid density is defined as $M_1 \times M_2$, $M_1 = 137$ and $M_2 = 137$. TP model transformation results in the rank of the discretized tensor $\mathcal{S}^D \in \mathbb{R}^{M_1 \times M_2 \times 6 \times 6}$, which is 2 in the first dimension and 3 in the second dimension. The weighting functions $w_{1,i}(U)$, $i = 1..2$, and $w_{2,j}(\alpha)$, $j = 1..3$, are depicted in Figure 1. The aeroelastic model (7) can be transformed exactly to finite element TP type polytopic model form with 6 vertex LTI models.

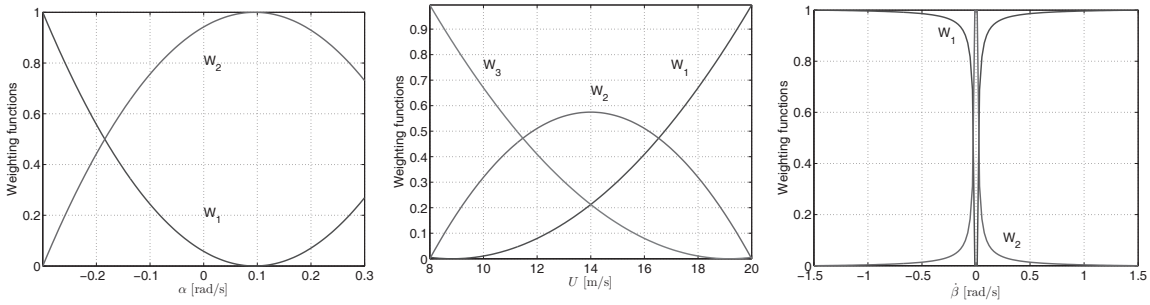

Fig. 1 CNO type weighting functions of the dimensions α and U. $\dot{\beta}$ is for the case, where nonlinear friction is included.

B. LMI based output feedback controller design

LMI-based control design can be immediately applied to the TP type polytopic form of the aeroelastic model (7) and the following controllers were designed:

1. Controller 1: Asymptotic stabilization and decay rate control

By applying Theorem 2, one finds that $\alpha = 0$ gives the best controller performance for the present model. This simply means that the LMIs in Theorem 2 become equivalent to the LMIs of Theorem 1.

2. Controller 2: Constraint on the control value

Two additional control solutions are also designed. In order to limit the bounds of the control values, Theorem 3 was applied. The minimal l_2 bound of the control value that still guarantees feasible LMIs was searched in the case of Controller 2.1-"min". For comparison, Controller 2.2-"max" was also derived, where a ten times larger bound limit of the control signal was applied.

C. Controller 3: Asymptotic state feedback control of the NATA model with nonlinear friction

The damping of the aeroelastic wing model in (3) has a linear viscous term. However, in many cases nonlinear friction models give more realistic description of the physical phenomenon, thus the linear viscous term is replaced by a Stribeck friction model in the present section. Simulation results showed that the previously designed controllers are not able to stabilize the NATA model with Stribeck friction. This comes from the fact that dimension of the nonlinearity increased. The aim of Controller 3 is to show how a given qLPV model can be extended with additional nonlinearities and how the controller can be derived systematically in a routine-like manner by applying the proposed control design strategy.

A Stribeck friction model defined in the following form is applied:

$$F_f(t) = -\left(F_c + \frac{(F_s - F_c)}{\left(1 + \left(\frac{v}{v_s}\right)^2\right)} \right) \text{sign}(v(t)) - F_v v, \tag{12}$$

where $c_{\beta_{servoC}} = 4.182 * 10^-4 Nm$ is the Coulomb friction term, $c_{\beta_{servoS}} = 1.2 \cdot c_{\beta_{servoC}}$ is the Stribeck friction term and $\dot{\beta}_{Stribeck} = 0.0075 rad/s$ is the Stribeck velocity. The values of these parameters were chosen based on engineering considerations in order to obtain a realistic friction model. It must be mentioned that other nonlinear friction models can also be implemented, which can be given in analytical, soft computing form or as data sets.

The parameter space Ω has to be extended by one dimension in $x_3(t) = \dot{\beta}$. The friction model is expected to be valid in the interval of $\dot{\beta} \in [-1.5, 1.5](rad/s)$. The grid density can be defined as $M_1 \times M_2 \times M_3$, $M_1 = 137$, $M_2 = 137$ and $M_2 = 138$ (even number for the grid in the third

dimension is chosen to avoid division by zero during discretization). The TP model transformation results CNO type TP polytopic model, the rank of the discretized tensor $\mathcal{S}^D \in \mathbb{R}^{M_1 \times M_2 \times M_3 \times 6 \times 6}$ is 2, 3, 2 in the first, second and third dimensions, respectively. The number of vertexes becomes $2 \times 3 \times 2 = 12$. The weighting functions can be seen in Figure 1.

State feedback Controller 3 for the above model was designed by applying the controller related terms of Theorem 1.

V. Numerical Experiment Results and Evaluation

A. Simulation

Numerical experiments are presented to demonstrate the performance of the designed stabilising control solution. Free stream velocity and $U = 14.1 m/s$ is chosen in order to be comparable to other published results. Open loop simulation was performed at the beginning of each test to let the oscillations fully develop. However, in the resulting figures, only that range of the simulation are shown where the controller is on.

Two simulation cases were compared for each controller.

- **Case 1 - perturbed system** is to test the robustness of the solution. Case 1 includes:
  - random noise normally distributed with a variance of 10% added to the measured output signal;
  - 3 ms constant time delay representing the computational delay;
  - modified nominal values of masses and inertia by $\pm 15\%$;
  - saturation of the control value.
- **Case 2 - ideal reference case** represents the ideal simulation cases without the perturbations listed in Case 1.

In case of Controller 3, Case 1 simulation has saturation of the control signal as the only perturbation.

Figures 2 and 3 show the time response of the controlled system for Controller 2.1 and 3, respectively.

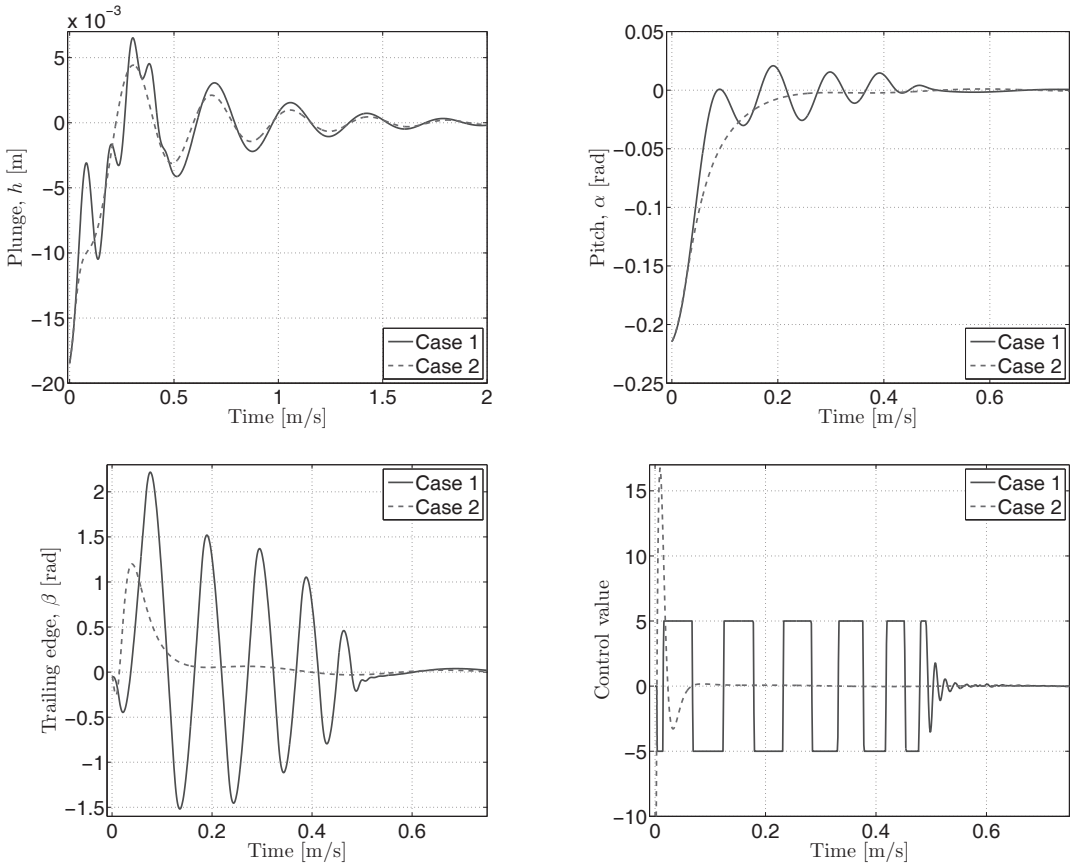

Fig. 2 Time response of Controller 2.1 for $U = 14.1m/s$.

Simulation for Controller 2.1 with sinusoidally varying free stream velocity are also performed, the results can be seen in Figure 4.

B. Evaluation

All of the designed controllers are able to asymptotically stabilize the state variables of the NATA model with linear and nonlinear friction. Controller 2.1 out of Controller 1, 2.1 and 2.2 has the smallest control signal amplitude in Case 2 and desaturates in 0.5 s, while the others desaturate in 0.9 s in Case 1. The settling times are similar for all of the controllers. Thus, it can be concluded that Controller 2.1 has the most favourable properties, therefore the simulation results of Controller 2.1 are given in Figure 2.

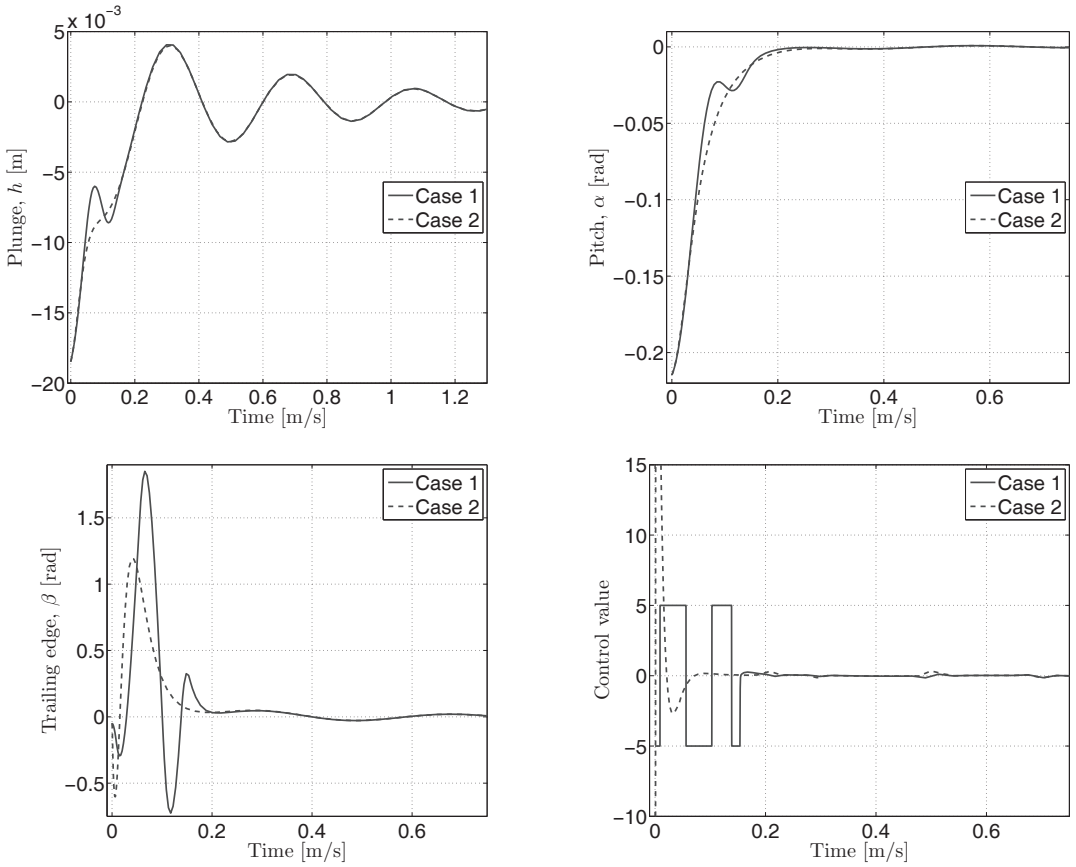

Fig. 3 Time response of Controller 3 for $U = 14.1m/s$.

1. Stability

An important issue should be addressed here. The applied LMIs guarantee that the resulting controller is stable. However, the TP model transformation is a numerical method that can be performed over an arbitrarily, but bounded domain Ω. Therefore, the stability ensured by the applied LMIs is restricted to Ω. Note that the accuracy of the given model is also bounded in reality for low speeds. The resulting controllers guarantee asymptotic stability in $\Omega : [-0.3, 0.3] \times [8, 20]$. One may extend Ω and execute the design method again. Controller 3 has an additional dimension in domain Ω, thus the stability domain becomes $\Omega : [-0.3, 0.3] \times [8, 20] \times [-1.5, 1.5]$.

2. Performance discussion

The control performance discussion focuses on two objectives based on the control performance specifications given previously. These are the maximal control values and the settling time for each

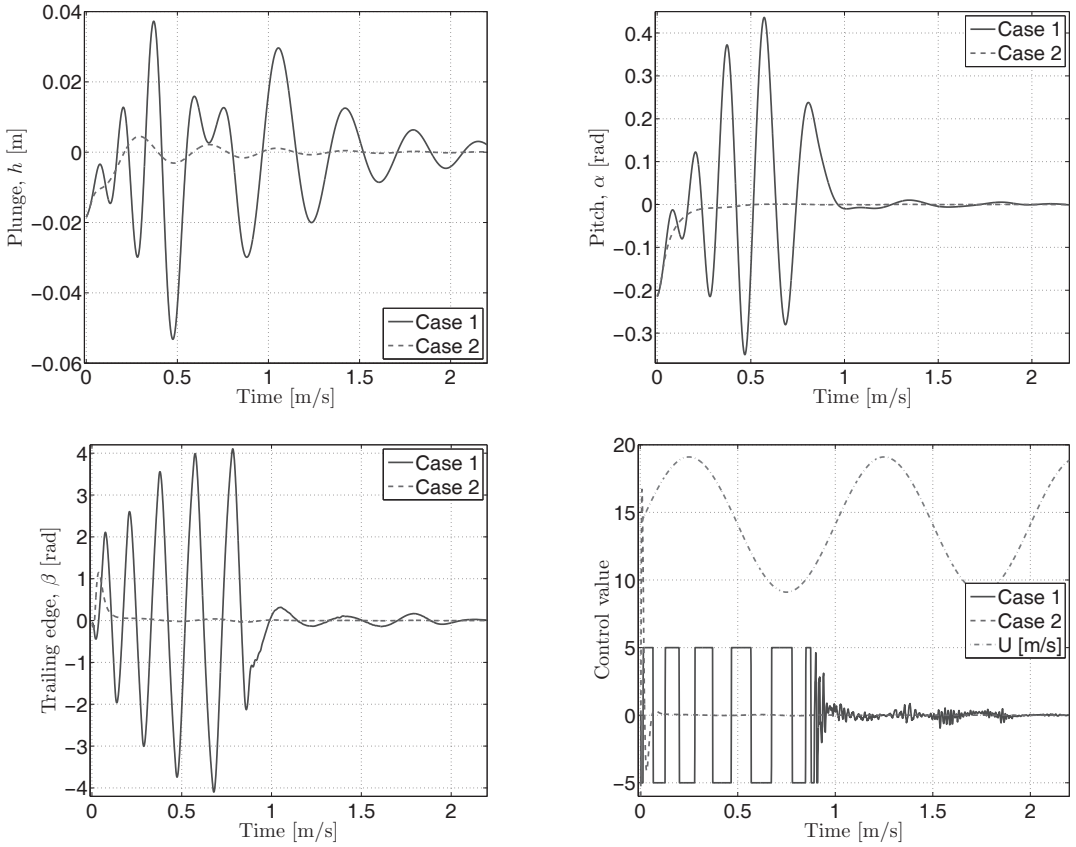

Fig. 4 Time response of Controller 2.1 with sinusoidally varying free stream velocity.

	Maximal control value	Settling time
Controller 1.1	Case 1: 5; Case 2: -350	Case 1: 1.5 s; Case 2: 1.5 s
Controller 2.1	Case 1: 5; Case 2: -15	Case 1: 1.5 s; Case 2: 1 s
Controller 2.2	Case 1: 5; Case 2: -60	Case 1: 1.5 s; Case 2: 1 s
Controller 3	Case 1: 5; Case 2: -14500	Case 1: 1.5 s; Case 2: 1.5 s

Table 1 Maximal control values and the settling times for the designed control solutions.

controller. The evaluation is summarized in Table 1.

It can be concluded that Controller 2.1 out of the first three designed controllers has the best performance according to our objectives. Controller 3 has a performance that is similar to Controller 1. However, Controller 3 has to stabilize the system with an additional nonlinearity caused by the friction.

3. Comparison with other results found in recent technical literature

Control performance: The control performance can be compared with the results presented in [15], where The LQR controller was designed for the same three DoF aeroelastic wing section. One can observe that the controllers derived with the TP type polytopic model and LMI design produce considerably faster responses in Case 2, but the cost is a higher control value. Case 1, which is a more realistic physical environment, saturates the control signal making the settling time somewhat longer, comparable to the results found in [15]. It also has to be mentioned that the LPV model in [15] has nonlinearity only in one dimension, namely in U, and the controller designed in the same paper is not output, but full state feedback controller.

A similar model was examined in [22] in which an LQR based output feedback controller was designed. The control performance is similar to the performance of Controller 2.1. However, simulation Case 1 of Controller 2.1 also includes time delay, parameter uncertainties and noise on the measured output signal.

The control performance, based on the above mentioned criteria, is similar to the controller presented in [9], which can be expected, since the same LMIs and the same control design methodology was used. On the other hand, it has to be emphasized that the present controller is designed for the three DoF model, rather than the two DoF model and the results of Case 1 simulations include time delay, noise on the measured signal, control signal saturation and parameter uncertainties.

Multi-input/multi-output control designs are used in papers [8, 12, 23]. However, the actuator dynamics are not included in the models in those cases.

Control design methodology: Note that very simple LMI theorems have been applied so far. If one would like to go for higher control performance, various choices of performance specifications could be attempted through more powerful LMI design theorems and further convex hull manipulation. Former solutions of the 3 DoF aeroelastic control problem do not focus on considerations other than stability.

VI. Conclusions

The proposed numerical control design methodology for Tensor Product type polytopic models can be executed systematically in a routine-like manner and preserves this property even if the model is extended with additional nonlinearities (such as friction). The proposed methodology is capable of control performance optimization through the use of linear matrix inequalities and convex hull manipulation. Based on the proposed control design methodology, the paper gives a stabilising control solution for the three degree-of-freedom aeroelastic wing section with linear and nonlinear friction. It is shown by simulation of a perturbed model that the designed controller and observer are resilient to a variety of perturbations. The next step of the research is to design a stabilising control solution to the same wing model with parameter uncertainties and the time delay included in the design phase and in the model, thus guarantees on the robustness can be made.

Acknowledgements

The research was supported by the Hungarian National Development Agency, (ERC-HU-09-1-2009-0004, MTASZTAK) (OMFB-01677/2009).

References

[1] Mukhopadhyay, V., "Historical Perspective on Analysis and Control of Aeroelastic Responses," *Journal of Guidance, Control, and Dynamics*, Vol. 26, Sept. 2003, pp. 673–684.

[2] Block, J. J. and Gilliat, H., "Active Control of an Aeroelastic Structure," *AIAA Meeting Papers on Disc*, American Institute of Aeronautics and Astronautics, Inc., Reno, NV, Jan. 1997, pp. 1–11.

[3] Block, J. J. and Strganac, T. W., "Applied Active Control for a Nonlinear Aeroelastic Structure," *Journal of Guidance, Control, and Dynamics*, Vol. 21, Nov. 1998, pp. 838–845.

[4] Mukhopadhyay, V., "Transonic Flutter Suppression Control Law Design and Wind-Tunnel Test Results," *Journal of Guidance, Control, and Dynamics*, Vol. 23, Sept. 2000, pp. 930–937.

[5] Strganac, T. W., Ko, J., and Thompson, D. E., "Identification and Control of Limit Cycle Oscillations in Aeroelastic Systems," *Journal of Guidance, Control, and Dynamics*, Vol. 23, Nov. 2000, pp. 1127–1133.

[6] Singh, S. N. and Wang, L., "Output Feedback Form and Adaptive Stabilization of a Nonlinear Aeroelastic System," *Journal of Guidance, Control, and Dynamics*, Vol. 25, July 2002, pp. 725–732.

[7] Platanitis, G. and Strganac, T., "Suppression of Control Reversal Using Leading- and Trailing-Edge Control Surfaces," *Journal of Guidance, Control, and Dynamics*, Vol. 28, May 2005, pp. 452–460.

[8] Reddy, K. K., Chen, J., Behal, A., and Marzocca, P., "Multi-Input/Multi-Output Adaptive Output Feedback Control Design for Aeroelastic Vibration Suppression," *Journal of Guidance, Control, and Dynamics*, Vol. 30, July 2007, pp. 1040–1048.

[9] Baranyi, P., "Tensor Product Model-Based Control of Two-Dimensional Aeroelastic System," *Journal of Guidance, Control, and Dynamics*, Vol. 29, March 2006, pp. 391–400.

[10] Baranyi, P., "Output Feedback Control of Two-Dimensional Aeroelastic System," *Journal of Guidance, Control, and Dynamics*, Vol. 29, May 2006, pp. 762–767.

[11] Prime, Z., Cazzolato, B., and Doolan, C., "A mixed H_2/H_∞ Scheduling Control Scheme for a Two Degree-of-Freedom Aeroelastic System Under Varying Airspeed and Gust Conditions," *Proceedings of the AIAA Guidance, Navigation and Control Conference and Exhibit*, Honolulu, Hawaii, 2008, pp. 1–16.

[12] Lee, K. W. and Singh, S. N., "Multi-Input Noncertainty-Equivalent Adaptive Control of an Aeroelastic System," *Journal of Guidance, Control, and Dynamics*, Vol. 33, Sept. 2010, pp. 1451–1460.

[13] Grof, P., Baranyi, P., and Korondi, P., "Convex Hull Manipulation Based Control Performance Optimisation," *WSEAS Transactions on Systems and Control*, Vol. 5, No. 8, Aug. 2010, pp. 691–700, Stevens Point, Wisconsin, USA.

[14] Takarics, B., Grof, P., Baranyi, P., and Korondi, P., "Friction Compensation of an Aeroelastic Wing - A TP Model Transformation Based Approach," *Proceedings of the IEEE 8th International Symposium on Intelligent Systems and Informatics SISY*, Sept. 2010, pp. 527–533.

[15] Prime, Z., Cazzolato, B., Doolan, C., and Strganac, T., "Linear-Parameter-Varying Control of an Improved Three-Degree-of-Freedom Aeroelastic Model," *Journal of Guidance, Control, and Dynamics*, Vol. 33, March 2010.

[16] Baranyi, P., Szeidl, L., Várlaki, P., and Yam, Y., "Definition of the HOSVD-based Canonical Form of Polytopic Dynamic Models," *3rd International Conference on Mechatronics (ICM 2006)*, Budapest, Hungary, July 3-5 2006, pp. 660–665.

[17] Baranyi, P., "TP Model Transformation as a Way to LMI Based Controller Design," *IEEE Transaction on Industrial Electronics*, Vol. 51, No. 2, April 2004, pp. 387–400.

[18] Baranyi, P., Szeidl, L., Várlaki, P., and Yam, Y., "Numerical Reconstruction of the HOSVD-based Canonical Form of Polytopic Dynamic Models," *10th International Conference on Intelligent Engineering Systems*, London, UK, June 26-28 2006, pp. 196–201.

[19] Scherer, C. W. and Weiland, S., *Linear Matrix Inequalities in Control*, DISC course lecture

notes, 2000, http://w3.ele.tue.nl/fileadmin/ele/MBS/CS/Files/Courses/DISClmi/lmis1.pdf, retrieved on 05.02.2012.

[20] Tanaka, K. and Wang, H. O., *Fuzzy Control Systems Design and Analysis: A Linear Matrix Inequality Approach*, John Wiley & Sons, Inc., 2001.

[21] Baranyi, P., "Convex Hull Generation Methods for Polytopic Representations of LPV Models," *7th International Symposium on Applied Machine Intelligence and Informatics, (SAMI 2009)*, Herlany, Slovakia, January 30-31 2009, pp. 69–74.

[22] Bhoir, N., "Output Feedback Nonlinear Control of an Aeroelastic System with Unsteady Aerodynamics," *Aerospace Science and Technology*, Vol. 8, April 2004, pp. 195–205.

[23] Wang, Z., Behal, A., and Marzocca, P., "Model-Free Control Design for Multi-Input Multi-Output Aeroelastic System Subject to External Disturbance," *Journal of Guidance, Control, and Dynamics*, Vol. 34, March 2011, pp. 446–458.